1 *Cross-sections*

The $K_L p \to \pi^+\Lambda$ and $K_L p \to \pi^+\Sigma^0$ are essential reactions to study the hyperon resonances - an analog of $N\pi$ reactions for the N^* spectra. They are also the key reaction to disentangling the weak exchange degeneracy of the $K^*(892)$ and $K^*(1420)$ trajectories. (A general discussion is given in Sections 13 and 9). The first measurement of this reaction was performed at SLAC in 1974 [1] for K^0 beam momentum range between 1 GeV/c to 12 GeV/c, which is shown in Fig.1. The total number of $\pi^+\Lambda$ events was about 2500 events, which statistically limits the measurement.

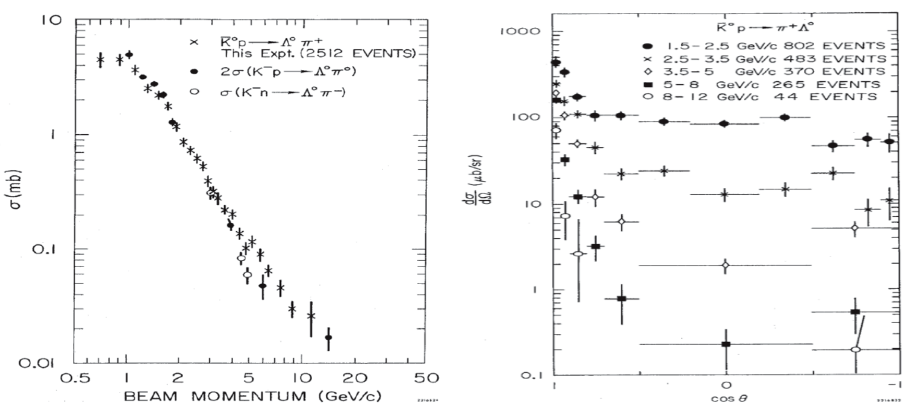

Figure 1: left panel: The total cross section for $K_L p \to \pi^+\Lambda$ reaction as a function of beam momentum [1] and right panel: The differential cross sections for various beam momentum ranges.

Figure 2 shows a single event of $K_L p \to \pi^+\Lambda$ with GlueX detector on GEANT simulation framework. Through the MC simulation, we show our estimate of the statistical uncertainty of the $\pi^+\Lambda$ total cross section as a function K_L beam momentum with GlueX detector in Hall-D as shown in Fig. 3. We kept the same momentum bin size as the one from the SLAC data. The box-shaped error bars in the MC points (red triangles) were increased by a factor of 5 for comparison with the SLAC data. The proposed measurements will provide unprecedented statistical accuracy to determine the cross section for a wide range of K_L momentum.

In figure 4, the t-dependent cross-sections were shown in three beam momentum bins same as SLAC data sets: p_{K^0}=1.5-2.5 GeV/c (solid bullets), p_{K^0}=2.5-3.5 GeV/c (solid rectangles)and p_{K^0}=3.5-5.0 GeV/c (solid triangles). As it shows, a strong forward peaking in t channel for all momenta was observed,

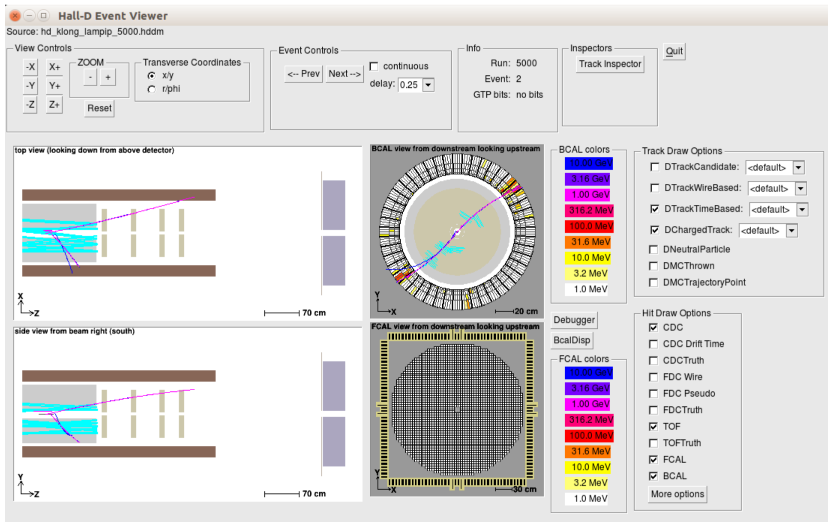

Figure 2: A sample of single event display of $K_L p \to \pi^+ \Lambda$ reaction with GlueX detector.

which appears to move out $\langle -t \rangle = 0.4$-0.5 GeV^2 at higher momenta. We expect K_L beam with GlueX data will provide precedent data with finer binning of t, which allows to confirm for the helicity non-flip dominance [2, 3, 4, 5].

2 *Polarization*

Parity violation in the weak decay of Λ makes it possible to measure the induced polarization. The induced Λ polarization (P_Λ) can be observed by measuring the angular distribution of the proton with respect to the normal vector to the production plane, which is given by Eq. (1).

$$I(\theta) = 1 + \alpha P_\Lambda \cos\theta \ , \tag{1}$$

where $\cos\theta = \hat{q}_p \cdot \hat{n}$, $\alpha = 0.645$, $\hat{n} = \hat{q}_i \times \hat{q}_f$. Here $\hat{q}_i$, $\hat{q}_f$, and $\hat{q}_p$ are the momentum unit vectors of the incident meson, outgoing meson and decay proton respectively in the Λ rest frame. At given a unit normalized probability distribution $I(z) = \frac{1}{2}(1 + az)$, where $z = \cos\theta$, the first momentum M_1 is defined as

$$M_1 \ = \ \int_{-1}^{+1} z \ I(z) \ dz \ = \ \frac{a}{3} \ . \tag{2}$$

Simply, αP_Λ is equal to $3M_1$. Therefore, $\alpha P_\Lambda = 3 \, \langle \cos\theta \rangle$ and its uncertainty is given by

$$\sqrt{\frac{3 - (\alpha P_\Lambda)^2}{N}}. \tag{3}$$

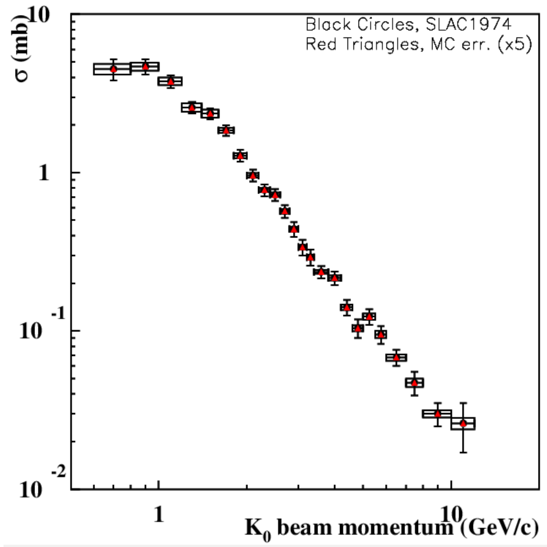

Figure 3: The total cross-section uncertainty estimate (statistical uncertainty only) for $K_L p \to \pi^+ \Lambda$ reaction as a function of K_L beam momentum in comparison with SLAC data [1]. The experimental uncertainties have tick marks at the end of the error bars. The box-shaped error bars in the MC points from K_L beam at GlueX were increased by a factor of 5.

From the SLAC data (Fig. 5) showed the results of polarization with the limited statistics. This pseudo data using our proposed K_L beam time shows how much uncertainty of polarization can be improved. Again, We kept the same momentum bin size as the one from the SLAC data. The box-shaped error bars in the MC points (red triangles). Figure 5 shows the beam momentum dependence: $p_{K^0} > 2.5$ GeV/c (red boxes), $p_{K^0} = 2.5 - 3.8$ GeV/c (blue triangles) and $p_{K^0} > 3.8$ GeV/c (purple bullets) for the averaged $\langle \alpha P_\Lambda \rangle$ over the momentum transfer region $-t = 0.2 - 1.0$ GeV^2. Overall, the data showed the momentum independence of $\langle \alpha P_\Lambda \rangle$, which is clear evident above the s-channel resonance region ($p_{BEAM} > 2$ GeV/c).

As shown in SLAC data there is a significant polarization at forward direction and peaking around $-t$=0.9 GeV^2 and falling slowly in larger $-t$, which indicates the s-channel helicity non-flip amplitude (f_{++}) dominance. This is similar polarization observation in $K^- N \to \pi \Lambda$ data. From a simple Regge formalism, the polarization is defined $P(s,t) = G(t)\ s^{\alpha_2(t) - \alpha_1(t)}$, where $\alpha_1(t)$ and $\alpha_2(t)$ are two highest trajectories exchanges.

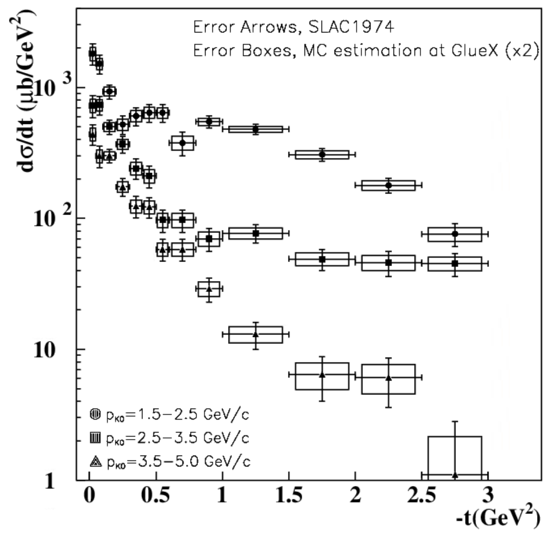

Figure 4: The differential cross-section as a function of t for three beam momentum bins from SLAC data. The box-shaped error bars in the MC points from K_L beam at GlueX were increased by a factor of 2.

A Details of MC study for $K_L\ p \to \pi^+\Lambda$

For our proposed KL Facility in Hall-D, we expect good statistics of $K_L p \to \pi^+\Lambda$ for a very wide range of K_L beam momentum. Figure 6 shows the KL beam momentum distributions from the generated (left) and reconstructed (right) with requiring $K_L > 0.95$ in time-of-flight.

We have generated the $K_L p \to \pi^+\Lambda$ reaction in phase space taking into account the realistic K_L beam momentum distribution in the event generator. This momentum spectrum is a function of the distance and angle. Then we went through the standard Hall-D full GEANT simulation with GlueX detector and momentum smearing. Finally, we utilized the JANA for particle reconstruction that we simulated. Figure 7 shows a sample plot for polar angle versus momentum distribution of π^+, π^-, and protons from the generated event (left) and reconstructed event (right).

Figure 8 shows an example of the reconstructed the particle for Λ invariant mass (left) and missing mass (right). We obtained a 5 MeV invariant-mass resolution and a 150 MeV missing-mass resolution. We estimate the expected total number of $\pi + \Lambda$ events as final-state particle within topology of $1\pi^+$, $1\pi^-$, and 1 proton. In 100 days of beam time with $1 \times 10^4 K_L/s$ on the liquid hydrogen target, we expect to detect around 3.5M $K_L p \to \pi^+\Lambda$ events for $W < 3$ GeV. Such an unprecedented statistics will improve our knowledge of these states through PWA.

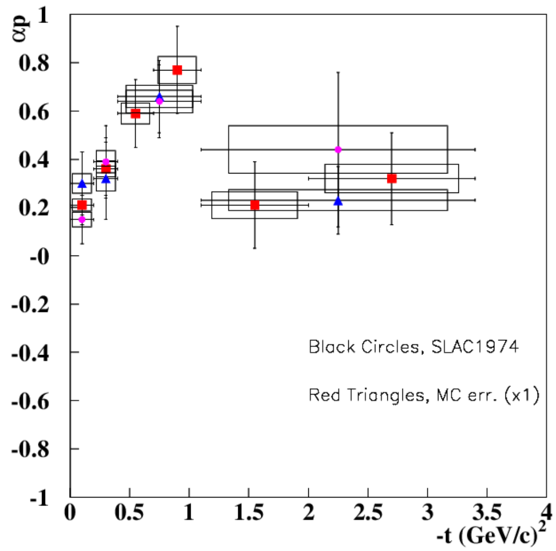

Figure 5: The averaged polarization, $\langle \alpha P_\Lambda \rangle$ as a function of the beam momentum, p_{BEAM} from Ref. [1], $p_{K^0} > 2.5$ GeV/c (red boxes), $p_{K^0} = 2.5-3.8$ GeV/c (blue triangles) and $p_{K^0} > 3.8$ GeV/c (purple bullets). The experimental uncertainties have tick marks at the end of the error bars. The box-shaped error bars from the MC.

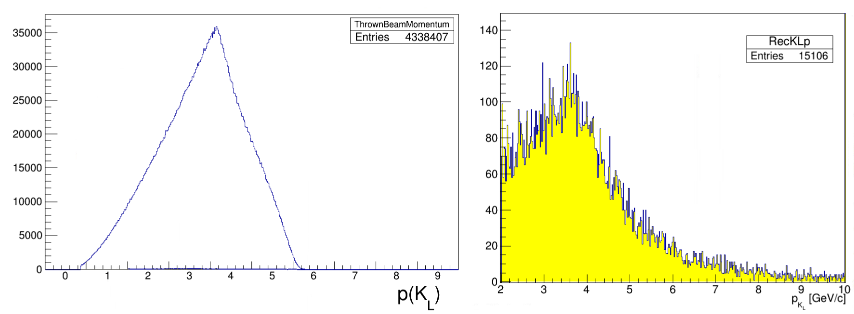

Figure 6: Beam particle (K_L) momentum distribution in MC simulation, left panel: Generated. right panel: Reconstructed.

Moreover, Fig. 9 (left) shows the correlation between invariant mass from its decay particles (p,π^-) and missing mass of $\pi^+ X$. The right plot in Fig. 9 shows the Λ invariant mass as a function of pion angular distribution (θ_{π^+}). All these plots are based on the 250 ps time resolution of the ST. The $K_L p \to \pi^+ \Lambda$ reaction has a relatively high production cross section the order of a few mb

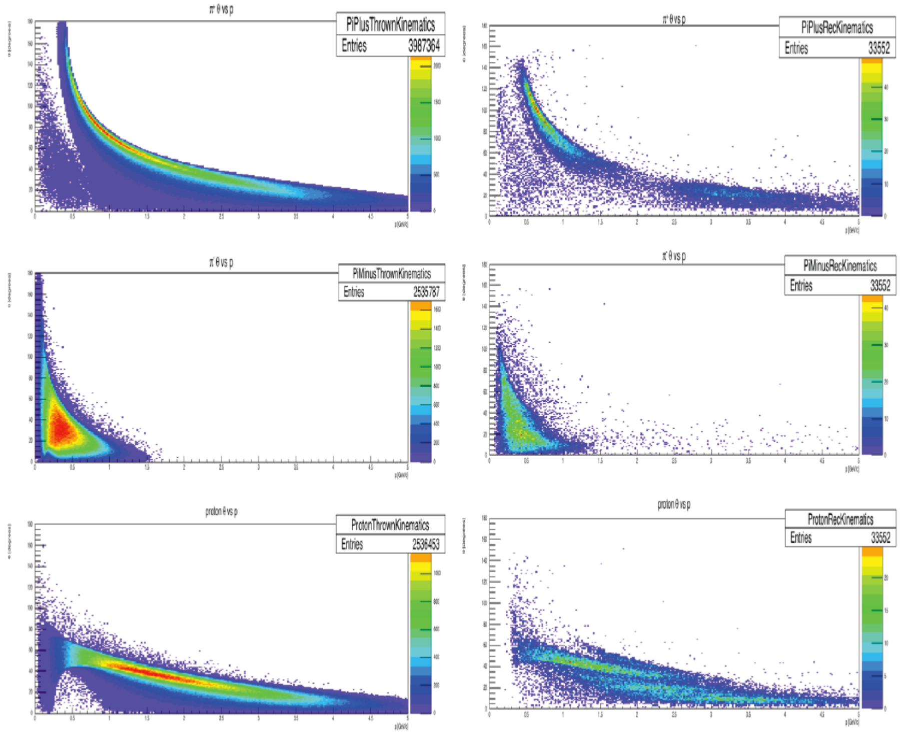

Figure 7: Momentum and angular distributions. top row panel: π^+, middle row panel: π^-, bottom row panel: proton. left column panels: Generated and right column panels: Reconstructed events.

in our proposed K_L momentum range (1 – 6 GeV/c). The beam momentum resolution has been improved by changing the flight path from 16 m to 24 m between Be-target and LH2 target. The variation of invariant-mass resolution as a function of W for various TOF-ST timing resolution (100, 150, 300 ps) is similar to those of other reactions [6]. The major source of systematic uncertainty for this reaction would be mistaken particle identification among π^+, K^+, and proton in the final state. However, requiring the reconstructed Λ and side-band subtraction technique for background will improve this uncertainty substantially.

References

[1] R. J. Yamartino Jr. SLAC-177 UC-34d (1974).

[2] J. S. Loos and J. A. J. Matthews, Phys. Rev. **D**6, 2463 (1972).

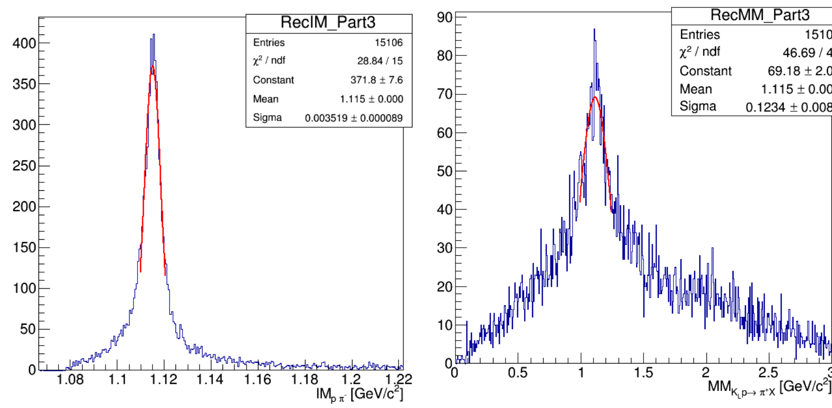

Figure 8: The Λ invariant-mass distribution reconstructed. left panel: From its $\pi^- p$ decay particles. right panel: The missing mass of $\pi^+ X$.

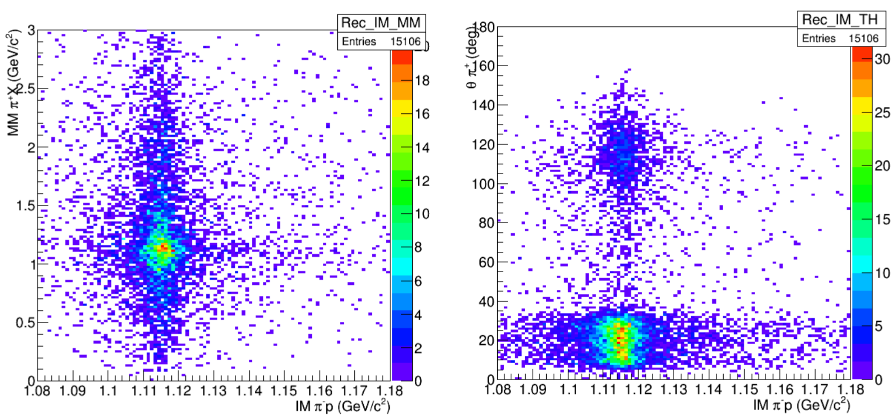

Figure 9: left panel: The Λ invariant mass versus missing mass of $\pi^+ X$. right panel: The θ_{π^+} angle distribution versus invariant mass.

[3] C. Michael and R. Odorico, Phys. Letts. **B**34, 422 (1971).

[4] A. C. Irving and A. D. Martin and C. Michael, Nucl. Phy. **B**32, 1 (1971).

[5] A. D. Martin, C. Michael, and R. J. N. Phillips, Nucl. Phys. **B**43, 13 (1972).

[6] KLong bi-weekly group meeting, https://wiki.jlab.org/klproject/index.php/March-1st, 2017.